Ročník 2013 electroscope Číslo V

The Possibility of Capturing Shock Waves by Computer Simulation in Environmental Scanning Electron Microscope

P. Vyroubal[1]
[1] Department of Electrical and Electronic Technology, Faculty of Electrical Engineering and Communication, BUT Brno,
Technická 10, Brno
E-mail: xvyrou02@stud.feec.vutbr.cz

Abstract:
Environmental scanning electron microscope (ESEM) is one of the latest trends in microscopic methods. In this microscope, we can observe various types of specimens, especially non-conductive and wet specimens. This is given by high pressure of gas in the specimen chamber. The evaluation of pressure on the secondary electrons trajectory is one of the important parameter in design of scintillation detector of secondary electrons. This article deals with computational modelling of pressure conditions and shock waves generation in the scintillation detector of secondary electrons for this type of microscope.

INTRODUCTION

Different signals are emitted from the specimen in the specimen chamber after the interaction with primary electrons (Fig. 1). Detector is a device used for the detection of the desired signal released from the specimen. Secondary electrons bring the information about the topology of the specimen.

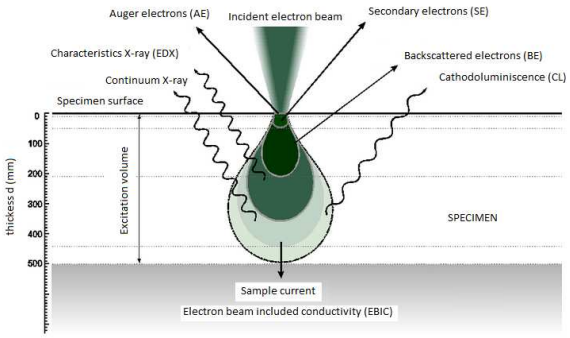

Fig. 1: Signals emitted by interaction between primary electron beam and specimen [1].

High pressure of gas in the specimen chamber makes impossible using the Everhart-Thornley detector, because high voltage must be placed on the scintillator. This voltage is used to acceleration secondary electrons on the scintillator. Principal scheme of scintillation detector is shown in the Fig. 2.

The area between specimen chamber and scintillator is separated by two apertures. Thanks to this, it is possible to create area by the scintillator with lower pressure than in the specimen chamber. Secondary electrons are accelerated by the voltage 8 kV. To avoid discharges in gas, the pressure 5 Pa must be in the area before the scintillator. Extraction and deflection electrodes E1 and E2 (voltage about hundreds volts) attract secondary electrons, which passes through to the apertures C1 and C1. Apertures C1 and C2 create electrostatic lens, because potential about hundreds volts is placed on them.

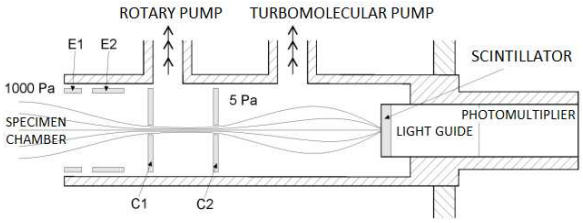

Fig. 2: The Principal scheme of scintillation detector of secondary electrons [2].

Electrodes and apertures are electrically isolated from the detector body. The area between apertures is pumped with the rotary pump, which serves to a gradual pressure reduction be-tween the specimen chamber and the chamber with scintillator. Behind the aperture C2, the area is pumped with the turbomolecular pump [2].

Scintillation detector consists of a scintillation crystal (YAG crystal, CRY 18, etc.), light guide and photomultiplier. After the absorption in scintillator, electrons generate a large number of photons, whose number is proportional to the energy of the electron. Part of these photons is brought to the photomultiplier, where photoelectrons are released. These electrons appear at the photomultiplier anode as an electrical impulse. Scintillation crystal and light guide are covered with reflective foil (e.g. Al). Suitable lubricant ensures optical contact between the scintillator and light guide. The lubricant prevents the losses of light reflection at the interface between two environments [3], [4].

MATHEMATICAL MODEL

For modelling the detector, SolidWorks software was used. The simulation of fluid flow was released by ANSYS Fluent software. ANSYS Fluent solves a system of three partial differential equations (law of conservation of mass, momentum and energy) completed with the fourth equation of state the considered fluid [5], [6], [7], [8], [9].

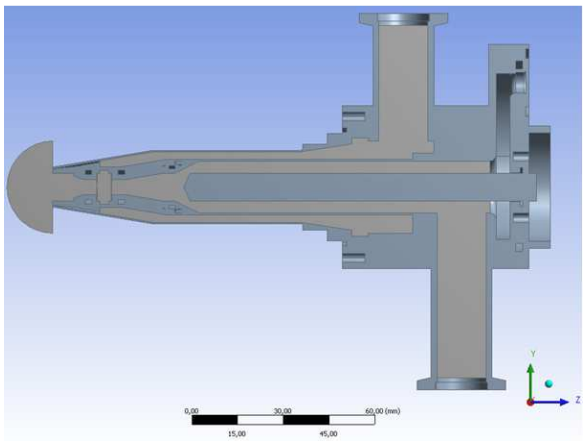

Fig. 3: Cross selection of the detector.

Continuity equation Eq. 1 expresses the law of conservation of mass and it takes the form:

$$\frac{\partial \rho}{\partial t} + \frac{\partial}{\partial x_i}\left(\rho u_i\right) = 0 \tag{1}$$

Navier - Stokes equations Eq. 2 express Newton's theorem applied to change of momentum in the form:

$$\begin{aligned} &\frac{\partial \rho u_i}{\partial t} + \frac{\partial}{\partial x_j}\left(\rho u_i u_j\right) + \frac{\partial p}{\partial x_i} = \\ &= \frac{\partial}{\partial x_j}\left(\tau_{ij} + \tau_{ij}^R\right) + S_i \end{aligned} \tag{2}$$

Energy equation Eq. 3 expresses the law of conservation of energy for compressible fluid and it takes the form:

$$\begin{aligned} &\frac{\partial \rho E}{\partial t} + \frac{\partial \rho u_i}{\partial x_i}\left(E + p\right) = \\ &= \frac{\partial}{\partial x_i}\left(u_j\left(\tau_{ij} + \tau_{ij}^R\right) + q_i\right) + \tau_{ij}^R \frac{\partial u_i}{\partial x_j} + \\ &+ \rho\varepsilon + S_i u_i + Q_H \end{aligned} \tag{3}$$

The equation Eq. 4 of state for the considered ideal gas, in the form:

$$\rho = \frac{p}{RT} \tag{4}$$

In the above equations u_i is fluid velocity, p fluid pressure, ρ fluid density, T temperature of the fluid, E the internal energy, S_i external mass forces acts per unit mass (gravity, centrifugal), Q_H supply and heat dissipation per unit volume, q_i flow heat, τ_{ij} viscous stress tensor and ij indexes indicate summation variables in three directions according to the coordinates (Einstein summation) [7], [9].

UPWIND COMPUTATIONAL SCHEME

In computational fluid dynamics, upwind schemes denote a class of numerical discretization methods for solving hyperbolic partial differential equations. Upwind schemes use an adaptive or solution-sensitive finite difference stencil to numerically simulate the direction of propagation of information in a flow field. The upwind schemes attempt to discretize hyperbolic partial differential equations by using differencing biased in the direction determined by the sign of the characteristic speeds.

Higher order upwind method captures better the areas with a higher gradient and correctly captures the strength of the shock waves. These schemes approximate solutions around the shock waves and the contact discontinuities. When the mesh is generated, the resulting flow field is not usually account [10].

Created mesh may be not optimal (e.g. in terms of capturing the gradient values), therefore an adaptation mode uses to improve the mesh. For adaptation mode is important, the correct criterion select for detecting for example shock waves.

First order upwind:

$$u_x^- = \frac{u_i^n - u_{i-1}^n}{\Delta x} \tag{5}$$

Second order upwind:

$$u_x^- = \frac{3u_i^n - 4u_{i-1}^n + u_{i-2}^n}{2\Delta x} \tag{6}$$

Third order upwind:

$$u_x^- = \frac{2u_{i+1} + 3u_i - 6u_{i-1} + u_{i-2}}{6\Delta x} \tag{7}$$

Finite volume/element method

For investigation of shock waves generated in the Laval nozzle ANSYS Fluent was used for approximation of results by the second order upwind method. The second order upwind method better

captures the areas with a higher gradient and correctly captures the strength of shock waves. The scheme approximates the solution well around shock waves and contact discontinuities [4]. ANSYS uses the finite element method.

The finite element method (FEM) (its practical application is known as finite element analysis FEA) is a numerical technique for finding approximate solutions to partial differential equations (PDE) and their systems, as well as (less often) integral equations. The method essentially consists of assuming the piecewise continuous function for the solution and obtaining the parameters of the functions in a manner that reduces the error in the solution. In simple terms, FEM is method for dividing up a very complicated problem into small elements that can be solved in relation to each other [11], [12].

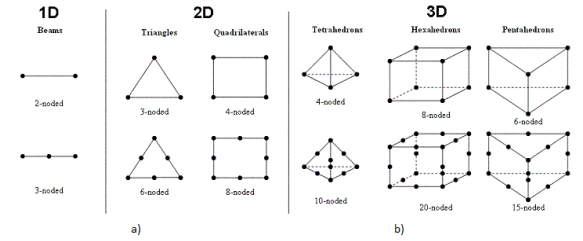

Fig. 4: Examples of (a) linear and (b) quadratic elements.

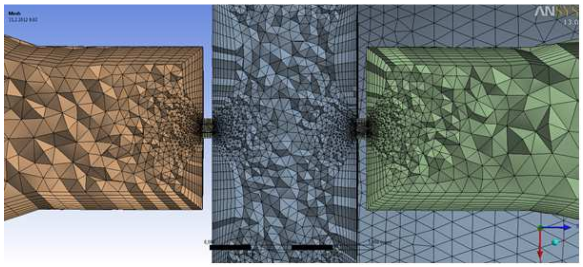

Fig. 5: The example of computational mesh.

RESULTS

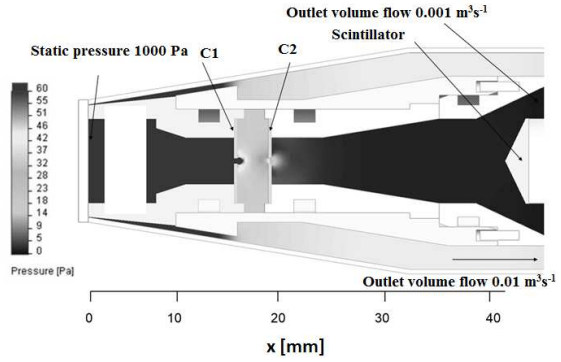

Fig. 6: The boundary conditions settings.

A supersonic flow created by apertures with circular orifices is accompanied by a local reduction in pressure (Fig. 8). This is an advantage in relation to the scattering of secondary electrons. There is a slight local decrease in pressure. Some energy is lost to the free expansion of gas around the nozzle mouth due to its geometry.

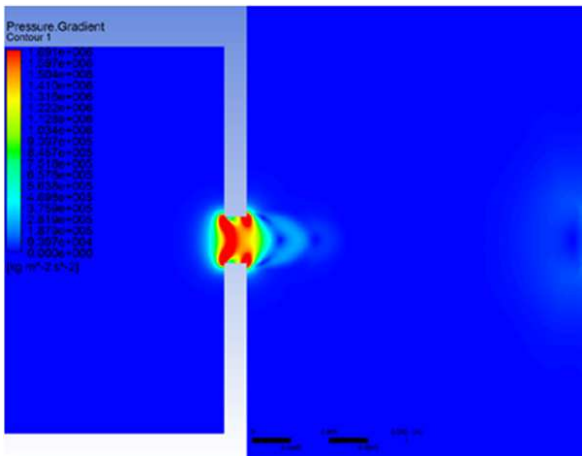

Fig. 7: Pressure gradient in the first aperture.

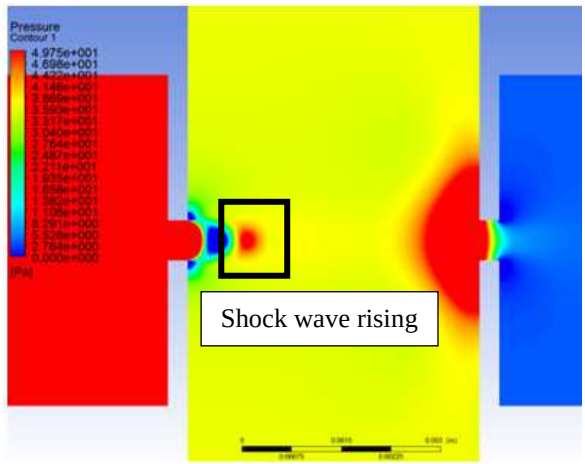

Fig. 8: Pressure condition in the detector and, the shock wave rising.

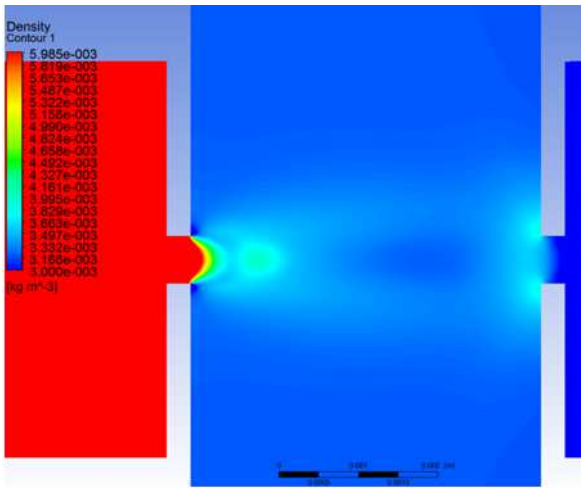

Fig. 9: Density change in the detector.

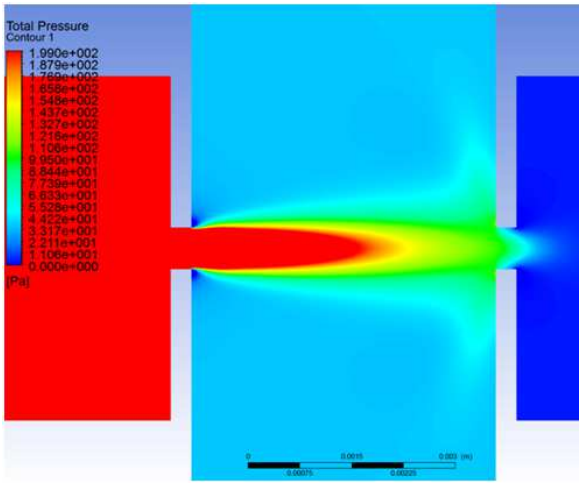

Fig. 10: Total pressure profile.

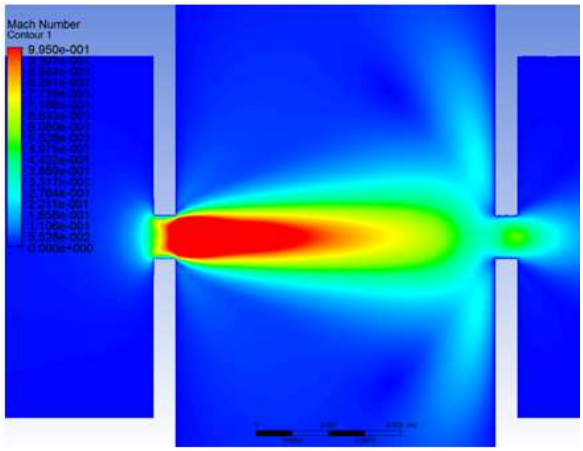

Fig. 11: Mach number profile.

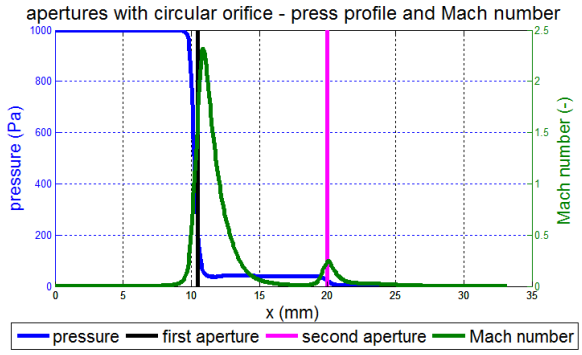

Fig. 12: Mach number and press profile across the detector.

The supersonic flow through the aperture can cause shock waves (Fig. 8). This is a significant compression of gas at short distances, which may create a barrier to the passage of electrons. The shock wave is a step change value (pressure, density), and it creates a discontinuity which in the calculations by the finite volume method cannot be described without a correct approximation type. The second order upwind method was used to investigate shock waves.

CONCLUSION

Shock waves are accompanying, but undesirable, phenomenon in the work of the microscope. Our aim is to eliminate this phenomenon. The possible solution is to explore and try out different combinations and sizes of the apertures.

Aperture C1 determines the pressure conditions across the detector. Gas that enters into it is moving into a critical state and moves at supersonic speed. Gas entering into aperture C2 is already moving at subsonic speed, far below the Mach number (Fig. 11 and Fig. 12).

Behind the apertures, swirls form in some cases that slow the pumping the area behind apertures. In some cases, swirls are formed directly in apertures or even before the entry into the first aperture, which again affects the pressure in the detector.

Although this work not demonstrated a direct shock wave formation in the detector, Fig. 8 and Fig. 9 shows pressure compression and density change behind the first aperture. It assumes that shock waves can occur in these places.

ACKNOWLEDGEMENT

This work was supported by the grant CVVOZE CZ.1.05/2.1.00/01.0014 and by the specific graduate research of the Brno University of Technology No. FEKT-S-11-7

REFERENCES

[1] ROUSHDEY, S.: Silicon Nano-cluster in Silicon Dioxide: Cathodoluminescence, Energy Dispersive X-Ray Analysis, Infrared Spectroscopy Studies, Crystalline Silicon - Properties and Uses, Prof. Sukumar Basu (Ed.), 2011, ISBN: 978-953-307-587-7

[2] JIRÁK, J., NEDĚLA, V., ČERNOCH, P., ČUDEK, P. and RUNŠTUK, J. Scintillation SE detector for variable pressure scanning electron microscopes. *Journal of Microscopy*, 2010, vol. 239, no. 3, p. 233-238. DOI: 10.1111/j.1365-2818.2010.03377.x.

[3] DANILATOS, G. Design and construction of an atmospheric or environmental SEM (part 3). *Scanning*, 1985, vol. 7, no. 1, p. 26-42. DOI: 10.1002/sca.4950070102.

[4] DANILATOS, G. Velocity and ejector-jet assisted differential pumping: Novel design stages for environmental SEM. *Micron*, 2012, vol. 43, no. 5, p. 600-611. DOI:10.1016/j.micron.2011.10.023.

[5] MAXA, J., NEDĚLA, V., JIRÁK, J., VYROUBAL, P. and HLADKÁ, K. Analysis of Gas Flow in a Secondary Electron Scintillation Detector for ESEM with a new system of Pressure limiting Apertures. *Advances in Military Technology*, 2012, vol. 7, no. 2, p. 39-44. ISSN 1802-2308.

[6] MAXA, J., NEDĚLA, V. and JIRÁK, J. Analysis of Gas Flow in the new system of Apertures in the Secondary Electron Scintillation Detector for ESEM. *Microscopy and Microanalysis*, 2012, vol. 18, supplement 2, p.1264-65. ISSN 1431-9276.

[7] FIALA, P. Pulse-powered virtual cathode oscillator. *Transactions on Dielectrics and Electrical Insulation*, 2011, vol. 18, no. 4, p. 1046-1053. ISSN 1070-9878.

[8] STRATTON, J. A. *Electromagnetic Theory*. New York: Mc Graw-Hill, 1941. 630 p.

[9] FIALA, P., FRIEDL, M. and SZABÓ, Z. EMHD Models Respecting Relativistic Processes of Trivial Geometries. *Progress in Electromagnetics*, 2011, vol. 2011, p. 96-99. ISSN 1559- 9450.

[10] HYMAN, M. and KNAPP, R. High Order Finite Volume Approximations of Differential Operators on Nonuniform Grids. *Physica D: Nonlinear Phenomena*, 1992, vol. 60, no. 1-4, p. 112-138. ISSN 0167-2789.

[11] VERSTEEG, K. and MALALASEKERA, W. *An Introduction to Computational Fluid Dynamics: The Finite Volume Method*. Reading, Addison-Wesley, 1995. 257 p.

[12] VYROUBAL, P. and MAXA, J. Analysis of the Impact of Supersonic Flow in Detector of Secondary Electrons ESEM. In *Proceedings 2nd Computer Science On-Line Conference*. Ithaca: Cornell University 2012, p. 149-155.